Electronic Supplementary Material (ESI) for Nanoscale.

Electronic Supplementary Information

Magnetic Properties of Core-Shell Nanoparticles Possessing a Novel Fe(II)-Chromia Phase: An Experimental and Theoretical Approach

Mohammad Delower Hossain[a], Robert A. Mayanovic[a†], Ridwan Sakidja[a], Mourad Benamara[b], Richard Wirth[c]

[a]Department of Physics, Astronomy & Materials Science, Missouri State University, Springfield, MO 65897.

[b]University of Arkansas Nano-Bio Materials Characterization Facility, University of Arkansas, Fayeteville, AR 72701, USA.

[c]GeoForschungsZentrum Potsdam, Department 3.3, Telegrafenberg, 14473 Potsdam, Germany

†RobertMayanovic@MissouriState.edu.

Characterization Procedures

X-ray photoelectron spectroscopy (XPS) analysis was performed on specimens of the CSNs using a twin-crystal monochromated Al Kα x-ray source having a characteristic energy of 1486.6 eV. The source and analyzer of the XPS instrument were calibrated using the Ag $3d_{5/2}$ (FWHM=0.36 eV) peak having a characteristic energy of 368.26 eV. An Alpha 110 hemispherical analyzer (Thermo Scientific) having a pass energy of 25 eV was used to collect the x-ray photoelectron spectra. The Casa XPS 2.3.16 software package was used for peak fitting analysis of the XPS spectra. Both the high resolution and survey scan were calibrated with respect to the C 1s peak (284.8 eV). The Shirley background and Gaussian-Lorentzian product GL(30) functions were used for the background and peak fitting, respectively. Transmission electron microscopy (TEM) samples were prepared by dispersing the α-Cr_2O_3@α-$Fe_xCr_{2-x}O_{3-\delta}$ CSNs in hexane followed by quick submersion of a carbon lacey grid into the CSN-suspended solution. The TEM images and TEM-based data were collected using a Titan 80-300 (FEI) instrument, with the field emission gun operated at 300 keV, located at the University of Arkansas Nano-Bio Materials Characterization Facility and using a G2 F20 X-Twin (TECNAI) microscope located at the GeoForschungZentrum, Potsdam, Germany. The emission gun of the G2 F20 X-Twin microscope was operated at 200 keV. ImageJ software was used for TEM image analysis.

Room-temperature x-ray diffraction (XRD) measurements were made using a D8 Discover (Bruker AXS) powder diffractometer. The instrument was operated at 40 kV and 40 mA using a Cu Kα radiation (λ = 0.154056 nm) x-ray source. A Gobel mirror with a 0.6 mm slit were used on the incident x-ray beam side whereas a Linxeye 1-D Si strip detector was used to measure the diffracted signal. Topas 4.2 software was used, along with the ICSD #173470 (space group #167) corundum structure, to accomplish Rietveld refinement of the XRD data measured from the CSNs. The modeling of the background of the XRD pattern was made using a Chebychev polynomial of 9-th order. The zero error and incident beam profile were modeled using the fundamental parameters profile fitting (FPPF) as implemented in Topas 4.2. We used a glass substrate to hold the CSNs, thus accounting for the amorphous-like background observed in the XRD pattern.

Results from Rietveld Refinement of XRD Data

Table S1: Summary of structural results obtained from Rietveld refinement for α-Cr_2O_3@α-$Fe_{0.40}Cr_{1.60}O_{2.92}$ CSNs.

Core: α-Cr_2O_3 (SG #167: $R\bar{3}c$); a = b = 4.960(1) Å; c = 13.576(4) Å ; V = 289.26(17) $Å^3$; core size = 26.1(15) nm					
Atoms	x	y	z	Site occupancy	B ($Å^2$)
Cr	0	0	0.3462(5)	1.0	0.6
O	0.313(5)	0	1/4	1.0	0.6
Shell: α-$Fe_xCr_{2-x}O_y$ (x=0.4; y=2.92) (SG #167: $R\bar{3}c$); a = b = 4.9617(17) Å; c = 13.623(4) Å ; V = 290.45(23) $Å^3$; core-shell size = 33(12) nm					
Cr	0	0	0.3418(7)	0.80	0.6
O	0.3169(62)	0	1/4	0.9733	0.75
O	0	0	0.366(2)	0.2	0.65

Additional TEM Results

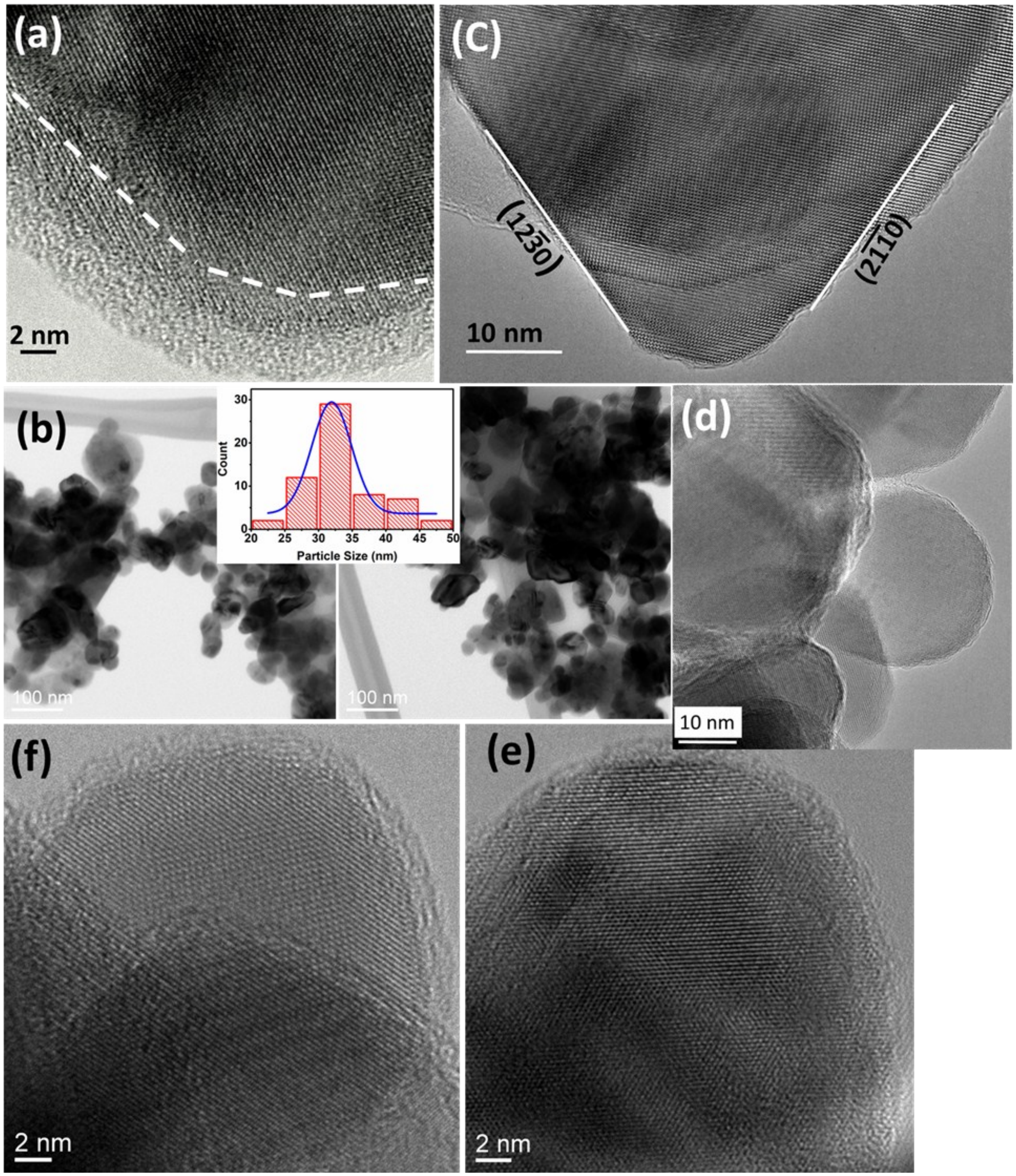

Figure S1. (a) HRTEM image of a CSN showing core-shell structure; (b) TEM images of the CSNs and a particle size distribution histogram plot; (c) a CSN showing the faceting of $12\bar{3}0$ and $2\bar{1}\bar{1}0$ planes; (d), (e) and (f) HRTEM images of different CSNs showing the particle morphology.

Figure S1 (a) shows the HRTEM image of a specific CSN where the core and shell are separated by an interface (white dashes). For this nanoparticle, the atomic registry of the core is maintained in the shell. The thickness of the shell region is ~2-3 nm. Figure S1 (b) shows a TEM image of CSNs used in part for particle size distribution analysis. Sixty different CSNs from different TEM frames were used for the particle size distribution analysis. The fit of the histogram plot gives a particle size of ~31.9(1) nm which is in good agreement with our XRD results. Figure S2 (c) shows the faceting of a CSN, along the $12\overline{3}0$ and $2\overline{11}0$ planes. The HRTEM images in Figure S1 (d) – (f) show examples of the spherical and quasi-spherical shape of our CSNs.

XPS Characterization of the Core-Shell Nanoparticles

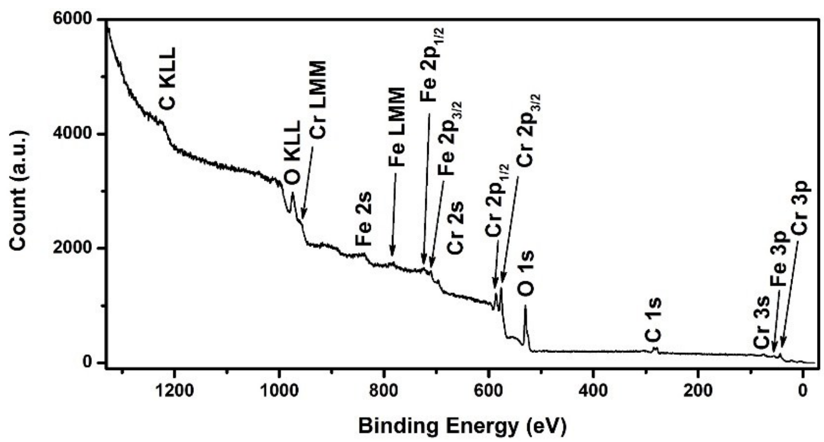

Figure S2. XPS survey scan analysis

Figure S2. shows the XPS survey scan of α-Cr_2O_3@α-$Fe_{0.40}Cr_{1.60}O_{2.92}$ CSNs. The survey scan analysis shows the presence of Fe, Cr and O in the sample. The C1s peak is from the tape used to hold the sample inside the XPS chamber. For elemental analysis of the CSNs $Cr2p_{3/2}$, O1s, $Fe2p_{3/2}$ peaks investigated and summary of the result are in Table S2.

Table S2. Summary of the result from XPS survey scan analysis of α-Cr_2O_3@α-$Fe_{0.40}Cr_{1.60}O_{2.92}$ core shell nanoparticles

Name	Position	FWHM	Area	Atomic%
$Cr2p_{3/2}$	575.73	4.17	3067.82	29.01
O1s	530.23	3.37	2735.41	67.88
$Fe2p_{3/2}$	709.73	3.60	462.91	3.12

Table S3: Summary of the result from high resolution XPS data analysis of α-Cr_2O_3@α-$Fe_{0.40}Cr_{1.60}O_{2.92}$ CSNs.

$Cr2p_{3/2}$		Position	FWHM	Line Shape	Area	%Area
Cr-O	Peak-1	572.37	2.30	GL(30)	379	6.43
	Peak-2	574.03	2.30	GL(30)	630.6	10.71
	Peak-3	575.55	2.30	GL(30)	2059.3	34.97
	Peak-4	576.56	2.30	GL(30)	1922.4	32.64
Cr-OH		577.64	2.30	GL(30)	898.6	17.77
O1s						
Fe-O		529.01	1.90	GL(30)	1321.3	14.89
Cr-O		530.27	1.90	GL(30)	3081.2	59.57
Cr-OH		531.79	2.28	GL(30)	770.3	14.89
Fe2p						
$Fe2p_{3/2}$		710.45	4.65	GL(30)	1549.4	66.84
$Fe2p_{1/2}$		723.69	5.00	GL(30)	768.7	33.16

Estimate of Fe Concentration in α-Cr_2O_3@α-$Fe_xCr_{2-x}O_y$ Core-Shell NPs

The calculation used to estimate the Fe concentration in the shell of our CSNs assumes a spherical shape of the nanoparticles for simplicity. Our analysis using an average ellipsoidal volume representation for the faceted nanoparticles is in very good agreement with the calculation using a spherical shape.

The average size of the CSNs is ~32 nm measured from TEM and XRD analysis and shell thickness is ~3 nm shown in HRTEM image (see Fig. 2(a)). In Fig. S3 we show a CSN model with $R = 16$ nm, $r_2 = 13$ nm (subtracting 3 nm for the shell), and $r_1 \approx 6$ nm (assuming ~10 nm of sampling depth for XPS). The ratio between the shell and XPS sampling volume z = (volume of shell)/(volume of the region accessed by XPS) ≈ 0.49.

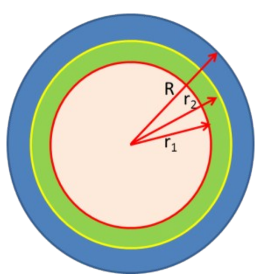

Figure S3. A schematic of a α-Cr_2O_3@α-$Fe_xCr_{2-x}O_y$ core-shell nanoparticle: R is the radius of the entire nanoparticle, r_1 is the radius of the volume of the nanoparticle excluded from XPS sampling ($r_1 = R -$ XPS sampling depth), and r_2 is the radius of the core of the nanoparticle ($r_2 = R -$ width of the shell).

From the XPS survey scan analysis, the atomic percentages of the elements were found to be as follows: Co:Cr:(O+OH) = 3.12:29.01:67.88. Excluding the contribution from OH^-, we get

Co:Cr:O = 3.12:29.01:46.64 for the stoichiometric chromate phase. Normalization of the contribution from the three elements gives ratios of Co:Cr:O = 3.96:36.83:59.21**.** Using the expression (1-z)•[Cr_2O_3] + z•[$Co_xCr_{2-x}O_3$] to find the concentration x in the XPS sampling volume, we can write:

0.0396[Fe] + 0.3683[Cr] + 0.5921[O] = (1 − 0.49)•{0.4[Cr] + 0.6[O]} + 0.49•{p[Fe] + (0.416 − p)[Cr] + 0.5839[O]}.

This yields, 0.0396[Fe] + 0.3683[Cr] = 0.407[Cr] + 0.49•p• ([Fe]-[Cr]) or p ≈ 0.0808. Thus, by stoichiometry, x = 5•p = 0.40. If, in addition, we account for the slight deficiency (~1.1 at%) of oxygen in the shell, we get $Fe_{0.40}Cr_{1.60}O_{2.92}$ as the approximate stoichiometric formula for the nanophase in the shell region of the core-shell nanoparticles (NPs).

UV-Vis Characterization of the Core-Shell Nanoparticles

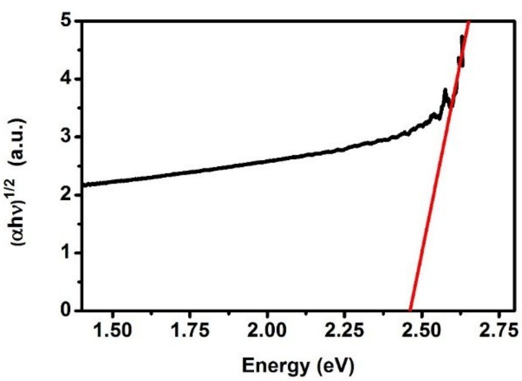

Figure S4. A Tauc plot made from a UV-Vis spectrum measured from α-Cr_2O_3@α-$Fe_{0.40}Cr_{1.60}O_{2.92}$ CSNs.

Magnetization Characterization of the Core-Shell Nanoparticles

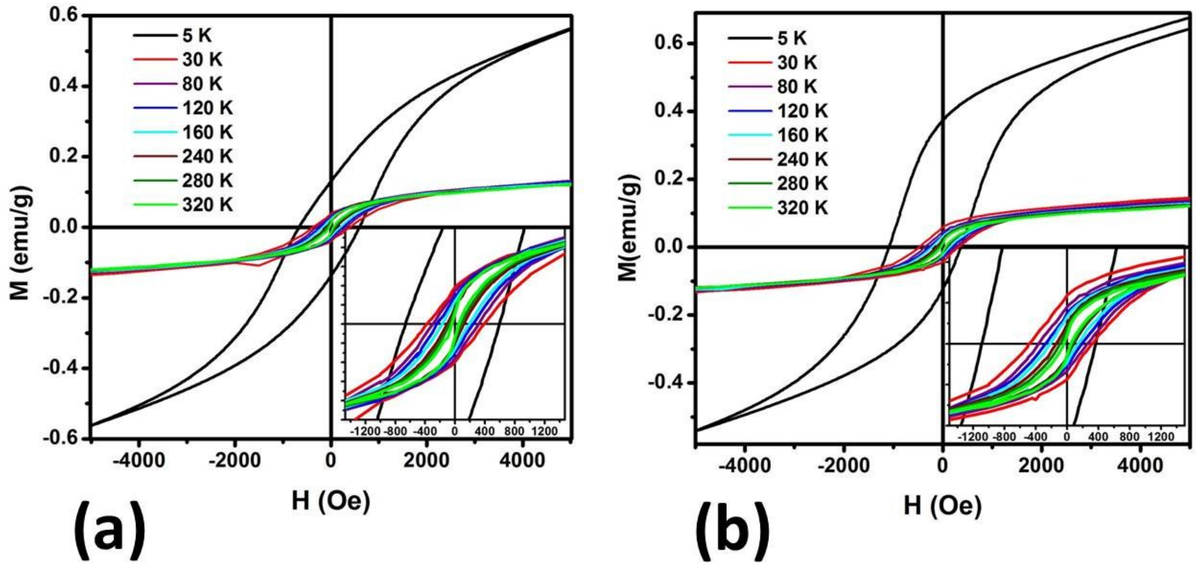

Figure S5. Hysteresis loop measurements made from α-Cr_2O_3@α-$Fe_{0.40}Cr_{1.60}O_{2.92}$ CSNs in the -5000 to 5000 Oe range, at temperatures ranging from 5 to 320 K for the (a) ZFC case and for the (b) FC case; the inset shows the region of each graph near H = 0 Oe. The M vs H data measured at 300 and 320 K, for both the FC and ZFC case, are nearly identical, hence only the 320 K data are shown.

Computational Results

Table S4: Magnetic moment (μ) values of atoms in α-Cr_2O_3 , α-Fe(III)Cr_3O_6 and α-Fe(II)Cr_3O_6

	μ (α-Cr_2O_3) (μ_B)	μ (α-Fe(III)Cr_3O_6) (μ_B)	μ (α-Fe(II)Cr_3O_6) (μ_B)
Cr1	3.11	2.98	3.07
Cr2	-3.11	-3.10	-3.09
Cr3/Fe	-3.11	-3.78	-3.46
Cr4	3.11	2.97	3.06
O1	0	-0.19	-0.10
O2	0	-0.17	-0.11
O3	0	-0.19	-0.10
O4	0	-0.14	-0.09
O5	0	-0.19	-0.10
O6	0	-0.17	-0.10

Table S5: Bader charge analysis of α-Cr_2O_3, α-Fe(III)Cr_3O_6 and α-Fe(II)Cr_3O_6.

Atom	Charge (α-Cr_2O_3) *e	Charge (α-Fe(III)Cr_3O_6) *e	Charge (α-Fe(II)Cr_3O_6) *e
O1	-1.6761	-1.59	-1.66
O2	-1.676	-1.58	-1.65
O3	-1.6925	-1.57	-1.64
O4	-1.6923	-1.61	-1.68
O5	-1.7137	-1.60	-1.67
O6	-1.7139	-1.61	-1.68
Cr1	2.5409	2.56	2.55
Cr2	2.5409	2.55	2.52
Cr3/Fe	2.5412	1.71	1.39
Cr4	2.5412	2.64	2.53

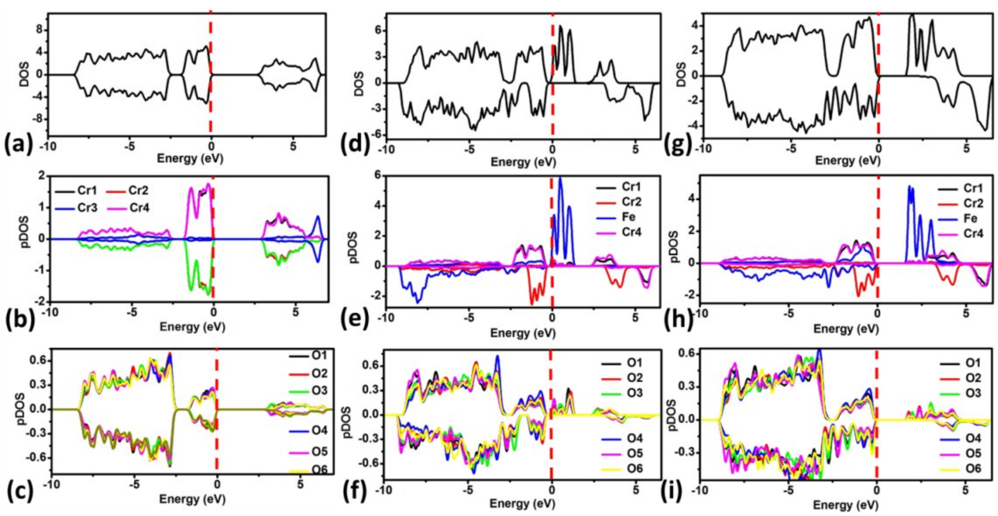

Figure S6. (a) DOS plot (b) and (c) pDOS plot of Cr 3d and O 2p of α-Cr_2O_3 ; (d) DOS plot and (e) pDOS plot of Cr and Fe 3d orbitals and (f) pDOS plot of O 2p of α-Fe(III)Cr_3O_6; (g) DOS plot and (h) pDOS plot of Cr and Fe 3d and (i) pDOS plot of O 2p of α-Fe(II)Cr_3O_6.

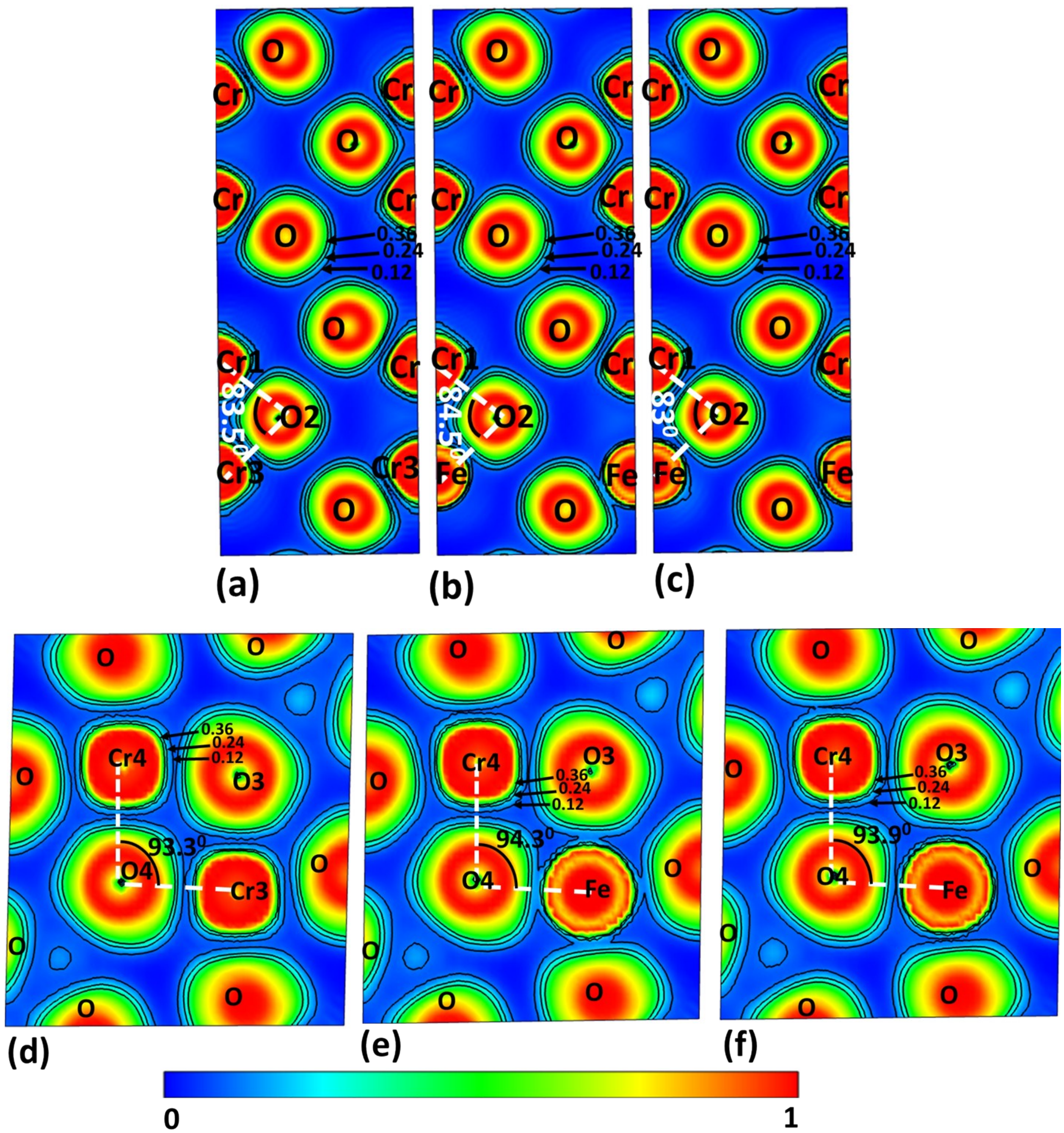

Figure S7. The ELF plot analysis along the $(10\bar{1}0)$ plane for (a) α-Cr_2O_3, (b) α-Fe(III)Cr_3O_6, and (c) α-Fe(II)Cr_3O_6; ELF plot analysis along the $(\bar{1}\bar{2}35)$ plane for (a) α-Cr_2O_3, (b) α-Fe(III)Cr_3O_6, and (c) α-Fe(II)Cr_3O_6.

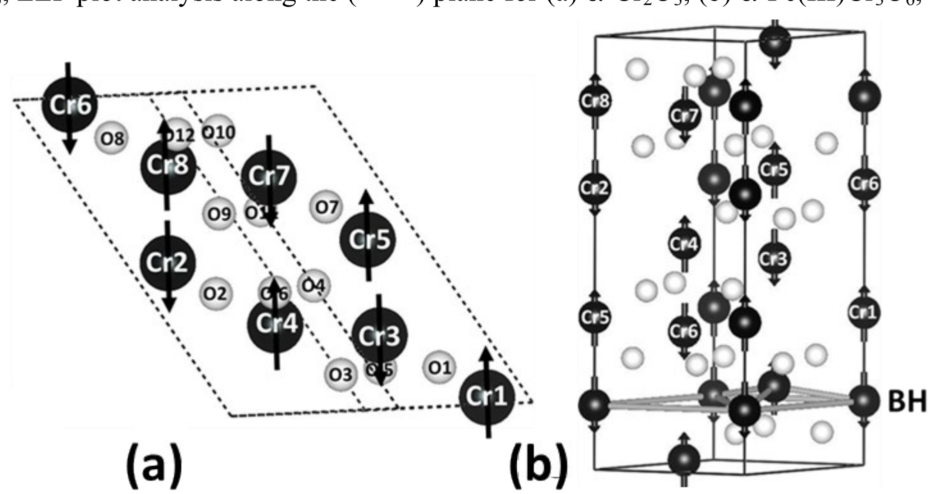

Figure S8. (a) The 1x1x2 supercell α-Cr_2O_3 structure (the different atomic positions are marked in the supercell along with the spin direction of the Cr atoms) (b) The full hexagonal α-Cr_2O_3 unit cell; atomic positions of the Cr's along with the spin directions shown in the 1x1x2 supercell in (a) are also shown in the hexagonal cell. BH indicates the buckled honeycomb (0001) plane.

Table S6: Equilibrium energy and corresponding magnetic moment values for several substitutional positions considered in the 1x1x2 supercell. The energy difference shown is with respect to the closest two Fe (Case-1) substitution in the cell.

Cases	**Substitution type**	**Initial Spin Configuration**	**Final Spin Configuration**	**α-Fe (III)$_2$Cr$_6$O$_{12}$**		**α-Fe(II)$_2$Cr$_6$O$_{12}$**		**Comment**
				ΔE (eV)/afu	**Magnetic Moment (μ_B)/afu**	**ΔE (eV)/afu**	**Magnetic Moment (μ_B)/afu**	
1	Fe3-Fe5	-+	-+	**0**	0	**0**	0	**closest pair along the c axis**
2	Fe3-Fe4	-+	-+	+0.002	0	+0.02	0	**Fe atoms in same BH plane & close to one another**
3	Fe4-Fe7	+-	+-	-0.02	0	-0.04	0	**both along c-axis and every alternate BH plane**
4	Fe3-Fe8	-+	-+	-0.02	0	-0.04	0	**Fe atoms in same BH plane & far apart from one another**
5	Fe4-Fe5	++	++	+0.009	0.99	+0.02	0.49	**Fe atoms in the (1114) plane & adjoining BH planes**
6	Fe4-Fe1	++	++	+0.009	1	+0.01	0.49	**one (0001) plane apart and farthest from each other**
7	Fe3-Fe7	--	--	-0.02	-0.98	-0.005	-0.49	**one (0001) plane apart and farthest from each other**

Table S7: Equilibrium energy, energy of formation of oxygen vacancy (E_{V_O}), and the magnetic moment values (per Fe site) calculated using the 2x2x2 supercell for Case 5 shown in Table S7 (Fe4 – Fe5 substitution), considered in the 1x1x2 supercell calculation, for the case of a single oxygen vacancy (V_O) created in either the O_{NN} or O_{NNN} positions.

Case	**Energy/afu (Ry)**	**E_{V_o} (eV)**	**Magnetic Moment (μ_B)/afu**
No V_O	-141.73979	--	0.503
V_O in O_{NN} site	-141.71910	4.51	0.381
V_O in O_{NNN} site	-141.71881	4.57	0.502

Fitting of the H_{EB} and H_C Data

Exponential equation: y = A1*exp(-x/t1) + y0

Linear equation: y = a + b*x

<table>
<tr><td rowspan="6">H_{eb}</td><td rowspan="3">Exponential</td><td colspan="2">y_0</td><td colspan="2">A1</td><td colspan="2">t1</td><td colspan="2">Statistics</td></tr>
<tr><td>Value</td><td>Error</td><td>Value</td><td>Error</td><td>Value</td><td>Error</td><td>Red. χ^2</td><td>Adj. R^2</td></tr>
<tr><td>41.29399</td><td>1.83377</td><td>391.79749</td><td>3.83894</td><td>25.18526</td><td>0.88485</td><td>0.2229</td><td>0.9996</td></tr>
<tr><td rowspan="3">Linear</td><td colspan="3">a</td><td colspan="3">b</td><td colspan="2">Statistics</td></tr>
<tr><td colspan="2">Value</td><td>Standard</td><td>Value</td><td colspan="2">Standard</td><td colspan="2">Adj. R^2</td></tr>
<tr><td colspan="2">117.84914</td><td>10.55896</td><td>-0.3722</td><td colspan="2">0.0389</td><td colspan="2">0.95769</td></tr>
</table>

<table>
<tr><td rowspan="6">H_c</td><td rowspan="3">Exponential</td><td colspan="2">y_0</td><td colspan="2">A1</td><td colspan="2">t1</td><td colspan="2">Statistics</td></tr>
<tr><td>Value</td><td>Error</td><td>Value</td><td>Error</td><td>Value</td><td>Error</td><td>Red. χ^2</td><td>Adj. R^2</td></tr>
<tr><td>101.6057</td><td>14.9353</td><td>668.07075</td><td>18.7986</td><td>71.17146</td><td>5.34429</td><td>205.1429</td><td>0.99546</td></tr>
<tr><td rowspan="3">Linear</td><td colspan="3">a</td><td colspan="3">b</td><td colspan="2">Statistics</td></tr>
<tr><td colspan="2">Value</td><td>Error</td><td colspan="2">Value</td><td>Error</td><td colspan="2">Adj. R-Square</td></tr>
<tr><td colspan="2">304.16379</td><td>8.26351</td><td colspan="2">-0.80733</td><td>0.03044</td><td colspan="2">0.99434</td></tr>
</table>